ResearchGate

See discussions, stats, and author profiles for this publication at: https://www.researchgate.net/publication/6843843

Proteomic Analysis of Amniotic Membrane Prepared for Human Transplantation: Characterization of Proteins and Clinical Implications

ARTICLE *in* JOURNAL OF PROTEOME RESEARCH · OCTOBER 2006

Impact Factor: 4.25 · DOI: 10.1021/pr050425q · Source: PubMed

CITATIONS
31

READS
43

5 AUTHORS, INCLUDING:

Andrew Hopkinson
University of Nottingham
63 PUBLICATIONS **782** CITATIONS
SEE PROFILE

Richard S Mcintosh
University of Nottingham
47 PUBLICATIONS **1,225** CITATIONS
SEE PROFILE

Patrick Tighe
University of Nottingham
106 PUBLICATIONS **2,542** CITATIONS
SEE PROFILE

Harminder Dua
University of Nottingham
349 PUBLICATIONS **7,624** CITATIONS
SEE PROFILE

Available from: Andrew Hopkinson
Retrieved on: 24 January 2016

research articles Journal of proteome research

Proteomic Analysis of Amniotic Membrane Prepared for Human Transplantation: Characterization of Proteins and Clinical Implications

Andrew Hopkinson,* Richard S. McIntosh,† Vijay Shanmuganathan, Patrick J. Tighe, and Harminder S. Dua

Division of Ophthalmology and Visual Sciences, University of Nottingham, United Kingdom

Received November 29, 2005

Amniotic membrane is commonly exploited in several surgical procedures. Despite a freeze preservation period, it is reported to retain wound healing, anti-angiogenic, antiinflammatory and anti-scarring properties; however, little is known about the active protein content. 2-DE analysis of transplant-ready amniotic membrane (TRAM) was performed. The effects of preservation and processing on amnion proteome were investigated, and the major proteins in the TRAM characterized using mass spectrometry and immunoblotting. This identified a spectrum of proteins including thrombospondin, mimecan, BIG-H3, and integrin alpha 6. Preservation compromises cellular viability resulting in selective elution of soluble cellular proteins, leaving behind extracellular matrix-associated and cell structural proteins. A number of key architectural proteins common to the architecture of the ocular surface were demonstrated in AM, which are involved in homeostasis and wound healing. Handling procedures alter the protein composition of amniotic membrane prepared for transplantation. Without standardization, there will be inter-membrane variation, which may compromise the desired therapeutic effect of transplant ready amniotic membrane.

Keywords: two-dimensional electrophoresis • amniotic membrane • thrombospondin • mimecan • βIG-H3 • ocular surface proteins

Introduction

The amniotic membrane (AM) is a component of the extra-embryonic tissue that surrounds the fetus, known collectively as the fetal membrane. AM has been used as a prosthetic material since the turn of the century[1] and its therapeutic applications are now considerably diverse. This includes acting as a resorbable barrier to prevent surgical adhesion,[2] as a substrate for nerve regeneration,[3] and as a prosthetic material for surgical reconstruction of the oral cavity,[4,5] bladder,[6] abdomen,[7] and vagina.[8] Perhaps most significant is its application in treating chemical and thermal burns.[9,10] More recently, the AM has found acceptance in the treatment of several ocular surface disorders, where it is utilized as a biological bandage (patch) or a substrate (graft) for epithelial growth.[11]

The mechanism(s) of action of AM is the subject of intense scrutiny. It is reported to possess anti-angiogenic, antiinflammatory, and anti-scarring properties which may be mediated by specific cytokines, notably growth factors, reviewed by Dua et al.[11] Conversely, it is suggested that the AM acts more as a biological scaffold, affording a viable basement membrane (BM) for epithelial cell growth and tissue repair.[11] The latter observations are pertinent when considering that AM is typically quarantined for six months for screening for transmissible diseases (e.g., HIV), usually involving a freeze preservation process. The effect of this process on protein composition and particularly on the beneficial clinical properties (e.g., wound healing) is unclear. Despite these concerns, there has been no accessible (or published) database of the AM proteome, which, if available, would greatly enhance our understanding of this tissue. The purpose of this study was to characterize proteins detected in transplant ready AM (TRAM), establish the effects of handling (processing, preservation, pre-operative preparation) on the proteome, and to identify key proteins which may play a role in the clinically beneficial effects of AM.

Material and Methods

Sample Procurement and Handling. Following ethical approval, human AMs were collected from consenting patients undergoing elective caesarean section, prepared for preservation according to published methodologies and stored at −80 °C for a minimum of 6 months.[12−14] Membrane segments were thawed and thoroughly cleaned by washing three times, in 10 mL saline containing protease inhibitors (complete protease inhibitor tablets, Roche, Lewes, UK), for 10 min each wash. Both the storage medium and the washes were retained, concen-

* To whom correspondence should be addressed. Division of Ophthalmology and Visual Sciences, University of Nottingham, EENT Centre, Queen's Medical Centre, Nottingham, UK. NG7 2UH. Tel: +115 9709796. Fax: +115 9709963.

† School of Biology, University of Nottingham, Nottingham, United Kingdom.

10.1021/pr050425q CCC: $33.50 © 2006 American Chemical Society
Published on Web 08/01/2006

trated by centrifugation and the proteins recovered, as described previously.[13]

Sample Solubilization. Protein extraction from membrane fractions was achieved by solubilizing 150 mg tissue, ground under liquid nitrogen, per 1 mL of lysis buffer (7 M urea, 2 M thiourea, 2%(w/v) CHAPS, 20 mM DTT (all Sigma, Poole, UK), 1%(v/v) IPG Buffer 3−11 NL (Amersham Biosciences, Little Chalfont, Bucks, UK), and protease inhibitors). Sample alkylation using *N*,*N*-dimethylacrylamide (DMA, Sigma) was performed using a final concentration 0.52%(v/v) DMA for 30 min followed by quenching the reaction with 20 mM DTT (final concentration) for 5 min (adapted from ZOOM IPG Runner protocols, Invitrogen, Paisley, UK). Samples were centrifuged at 21 000 × *g*, 4 °C, 45 min to remove insoluble material.

Two-Dimensional Electrophoresis. 2-DE was carried out according to published methodologies.[13] Protein was subjected to precipitation (2-D cleanup kit, Amersham Biosciences) according to the manufacturers protocol (revision 80−6486-60/Rev. CO/11−02). 18 cm Immobiline DryStrips pH3−11NL (Amersham Biosciences) were rehydrated according to manufacturers recommendations, using 7 M urea, 2 M thiourea, 2%-(w/v) CHAPS, 125 mM Bis(2-hydroxyethyl) disulfide (HED) (Sigma), 0.5% IPG buffer pH3−11 (Amersham Biosciences) and 0.002%(w/v) bromophenol blue. Rehydrated strips were transferred to the Ettan IPGphor manifold (Amersham Biosciences) and 65 μg samples (in a maximum volume of 100 μL) were anodic cup-loaded according to the manufacturers protocol. Focusing was carried out using the following parameters, 30 V for 1.5 h; 180 V (10 V per cm field strength) for 3 h; 300 V, step and hold, 3 h; 1000 V, gradient, 6 h; 8000 V, gradient, 3 h; 8000 V, Step and Hold, 3 h). Focused IPG strips were equilibrated for 5 × 3 min in 2 mL of equilibration buffer containing 6 M urea, 2%(w/v) SDS, 1%(w/v) DTT, 30%(v/v) glycerol (all Sigma), 50 mM Tris-HCl pH8.8, 0.01%(w/v) bromophenol blue, followed by a second equilibration step replacing DTT with 250mM Iodoacetamide (IAA; Amersham Biosciences). SDS-PAGE was performed using 20 cm polyacrylamide (30%(w/v) acrylamide: 0.8%(w/v) Bis-Acrylamide, 37.5:1 stock, National Diagnostics, Hull, UK) gradient gels (8%-19%) using the PROTEAN plus Dodeca system (Bio-Rad, Hemel Hempstead, UK). Protein visualization was performed using a modified silver stain procedure compatible with mass spectrometry.[15]

Image Analysis. Stained gels were imaged using a GS-800 calibrated densitometer followed by quantitative analysis using PDQuest software v.7.1.1 (both Bio-Rad), which uses Gaussian calculations. Under ideal conditions, the bivariate Gaussian model represents diffusion of an initial concentration focused at a single point in two independent directions.[16] Spots were matched between gels within a replicate group for each sample to obtain a consensus match, and then among all gels thus generating a synthetic master image containing the composite spot data from all the gels in the analysis set. The correlation coefficient (CC), ranges from 0 to +1, and indicated variation between a member and the master, with 0 being most variable and 1 being identical. The coefficient of variation (CV) indicated the relative variability between a consensus group (matched composite of the replicate gels for each sample) and the master.

Mass Spectrometric Identification of Protein Spots. Individual spots were excised using a 1.5 mm One Touch Gel Spot Picker (Web Scientific Ltd, UK) from preparative 2-D gels and de-stained. Proteins contained within a spot were reduced with DTT, alkylated using IAA and digested with trypsin[17]. For peptide mass fingerprint (PMF) analysis, peptide mixtures eluted and isolated (ZipTip tip, Millipore Corporation) from each gel spot were analyzed by MALDI-TOF−MS (Waters/Micromass, Elstree, UK), operating under MassLynx 4.0, at >8000 resolution (full width half-maximum [fwhm] definition) in reflection mode, according to manufacturer's instructions. Spectra were acquired at 5 Hz using a nitrogen laser with 10 shots per spectrum. The spectra were processed (deisotoped, background subtracted, smoothed using the Savitzky Golay model and centered) to generate singly charged monoisotopic masses. A negative control taken from a region of spot free gel was used to generate a list of contaminant ions, which, together with a list of known keratin and tryptic autolysis fragments, were excluded from the peak list. The peak lists were used to query all human MSDB and Swiss-Prot entries using Mascot peptide mass fingerprint online; http://www.matrixscience-.com/search_form_select.html (Matrix Sciences, London, U.K). The PMF searches were performed using a peptide tolerance of ±0.2 Da and only identifications based on at least 4 peptide matches were accepted. To validate the accuracy of PMF identifications, the searches were repeated against a randomized sequence database (Mascot, Matrix Sciences), only accepting identifications with randomized scores below the significance threshold. For MS/MS analysis, peptides were individually fragmented by nano-ESI-Q-TOF−MS/MS (Waters/Micromass). After data acquisition, the MS/MS spectra were combined, smoothed, deisotoped, and the de novo sequences manually assigned from daughter ion spectra using BioLynx section of the MassLynx software package. The generated peptide sequences and peak mass lists were used to query all human MSDB and Swiss-Prot entries using Mascot sequence query (Matrix Sciences). All searches were performed at a peptide tolerance value of 0.6 Da, and a MS/MS tolerance of 0.8 Da. Only peptides produced by trypsin (allowed up to 1 missed cleavage) were considered. To normalize data only scores from Swiss-Prot (release 48.4, 254527 sequences; 115605601 residues) are reported, and only identifications based on a score more than 60 were accepted as being significant ($p<0.05$).

Western Blots. 1-D SDS-PAGE was performed by separating solubilized protein, under denaturing and reducing conditions, using 12 well NuPAGE Novex 4−12% Bis-Tris gels (Invitrogen), according to manufacturer's protocol. Western blot analysis was carried out using the Novex XCell II Blot module (Invitrogen) for protein transfer, onto Immobilon Psq PVDF (polyvinylidene fluoride, Millipore, Watford, UK) membranes according to manufacturer's protocol. Membranes were blocked for 1 h at room temperateure using Tris buffered saline pH8.0 (Sigma), 0.05%(v/v) Tween 20 (Promega, Southampton, UK), and, 1% (w/v) nonfat milk powder (TBSTM) followed by immunodetection of human thrombospondin 1 (TSP-1) using mouse monoclonal anti- human TSP-1 (AB-11, NeoMarkers, LabVision, UK) antibody. Antibody Ab-11 was a cocktail of three monoclonal antibodies (Clone D4.6 + A6.1 + MBC 200.1) targeted to different domains of the TSP-1 structure; Clone D4.6 targeted against Calcium ion binding domain; Clone A6.1 targeted against Collagen Type V-binding domain; and, MBC 200.1 targeted against the N-terminal HBD. Primary antibody was detected using alkaline-phosphatase conjugated goat anti-mouse IgG (H+L), (preadsorbed to bovine, horse, human antibodies, Pierce, Cheshire, UK). Blots were developed with premixed 5-bromo, 4-chloro,3-indolyl phosphate(BCIP)/ni-

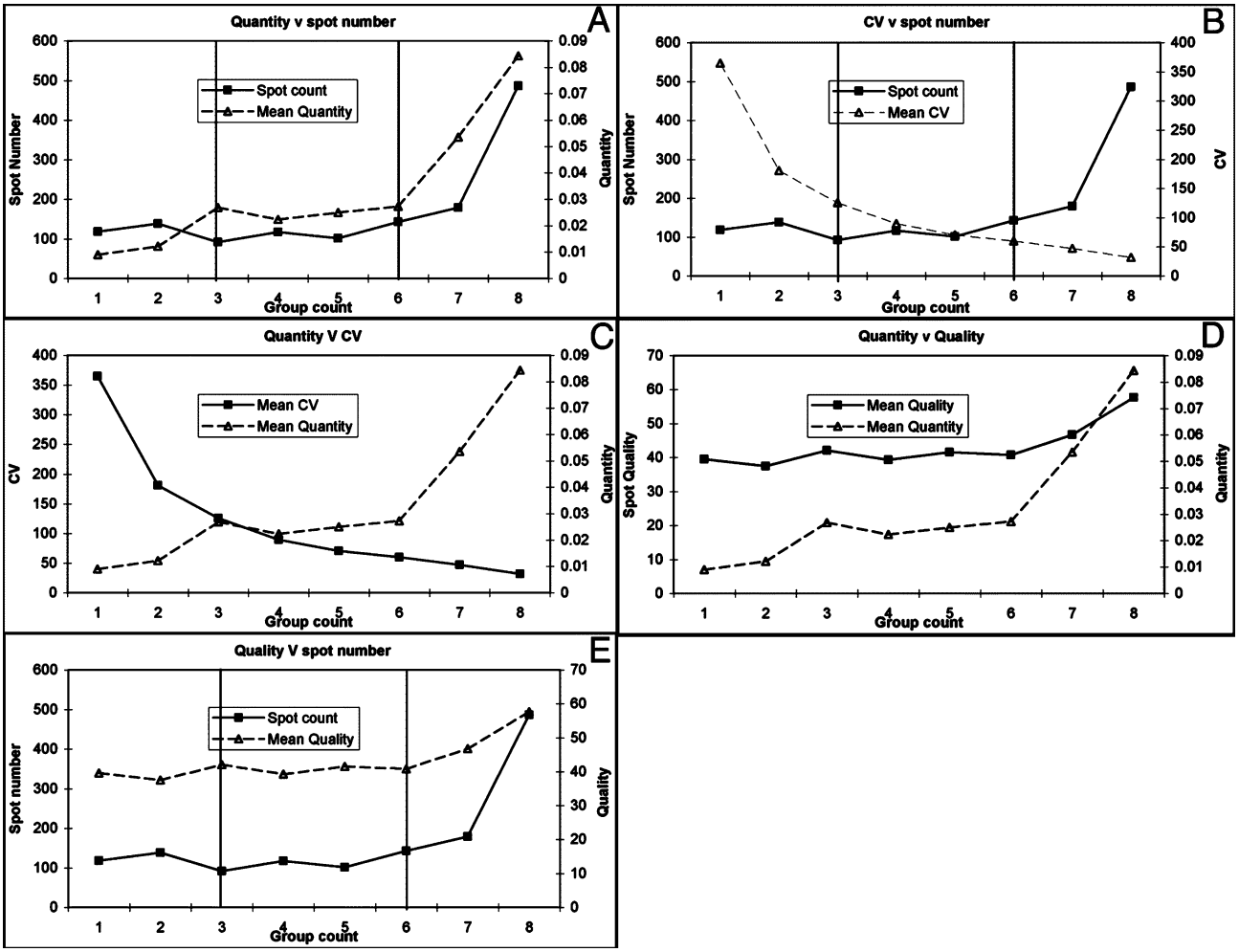

Figure 1. 2-D data analysis of TRAM. Spots were assigned to one of the eight groups depending on how many membranes out of a total 8 replicate groups of 3 gels (24 gels) they were detected in (group count; *x*-axis). The number of spots in each group (spot number), mean quantity of each spot (standard error range 0.0001−0.0007), mean spot quality (standard error range 0.046−0.181) and mean CV (standard error range 0.03−0.3) were plotted for each group of spots to allow the relationship between these statistical measures to be determined. The mean spot quantity is plotted with mean abundance (panel A), CV (panel C) and mean quality (panel D). The spot number for each group (spot abundance) is plotted with mean quantity (panel A), mean CV (panel B) and mean quality (panel E).

troblue tetrazolium (NBT) (Sigma). Platelets contain large amounts of TSP-1 therefore protein extracted from platelets was used as the positive control for TSP-1 antibody reactivity.

Results and Discussion

Before compiling the 2-D map, a highly standardized procedure for reproducibly extracting and resolving AM proteins was developed from previously published methodologies.[13] Membranes were handled and prepared for surgery according to established procedures.[12] Protein extracts from the TRAM and corresponding wash media were prepared, and 2-DE was carried out. Analysis of fresh AM was not carried out, as a previous study showed that combined analysis of TRAM and eluted fractions included all proteins detected in fresh AM.[13]

Assessment of Intra-Sample Gel-to-Gel Reproducibility. 2-DE was performed in triplicate on each sample extracted from eight different TRAMs. Technical variability can be introduced at various stages through a large-2-D gel based approach.[18] To minimize this, the procedure was rigorously standardized (supplemental information "2-D Standardization") and replicate gels (three per sample) from individual samples were run and analyzed concurrently. Analysis of replicate gels (triplicate gels for each membrane sample) detected an average of 1043 (range: 746 to 1228) silver stained specific protein spots across all consensus groups, but with a matching efficiency of approximately 99% between the replicate gels of a single consensus. A high average correlation coefficiency (CC) of 0.884, and a low average mean CV (MCV) of 40 implied good intra-sample reproducibility.

Inter-Sample Data Analysis for TRAM. Inter-sample cross matching detected an average of 946 (range: 832 to 1069) spots across 24 2-D gels representing eight TRAMs run in triplicate. Spot matching revealed an average efficiency of 69%, (average CC 0.838, and MCV of 61.23), suggesting some variation between different membranes. However, a Friedman test showed that the variation was not significant enough ($P = 0.0639$) to reject the null hypothesis that all TRAM were not the same. To validate these findings, spot data was further analyzed using the microarray analysis software package TMEV (http://www.tigr.org/). Initial analysis grouped all gels together confirming the samples were of the same biological origin. However, more detailed analysis clustered together the triplicate set of gels for each membrane, revealing many subtle variations between membranes.

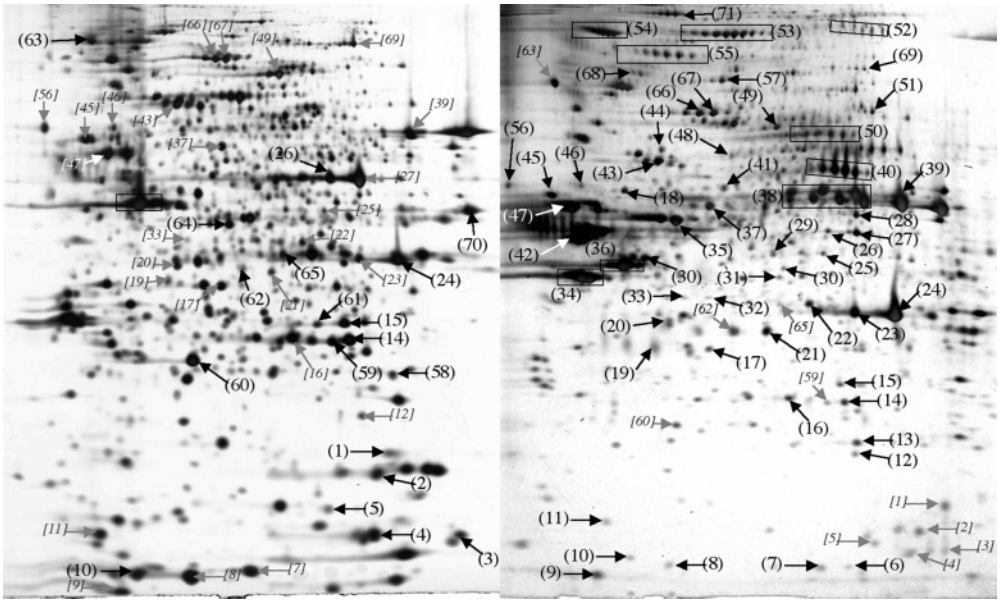

Figure 2. 2-D gels of wash media and TRAM. 2-DE analysis of solubilized protein derived from concentrated pooled wash media (A), and TRAM (B). 75 μg of protein was separated on 18 cm pH3−11 IPG strips (Amersham Biosciences) and then on 8−19% gradient polyacrylamide gels followed by silver staining. The spots indicated were identified using mass spectrometry (see Tables 1 and 2 for spot details, and Supporting Information Figures 1 and 2 for mass spec data).

Spots were assigned to one of eight groups depending on the number of membranes (1−8) in which they had been detected (spot abundance). Analysis of this grouping revealed that as abundance increased, spot quantity also increased (Figure 1, A) and variability (CV) decreased (Figure 1B). An inverse relationship between spot variability and quantity was therefore apparent (Figure 1C), with spot quality remaining largely consistent in all groups (Figure 1D and E). Spots detected in all eight membranes accounted for 35% of all spots detected. Conversely, the least abundant spots (detected in <3 groups) bordered the threshold of detection (low quantity; Figure 1D), suggesting experimental variation in the detection system rather than true intra-membrane variation is responsible for the detectable differences between TRAMs. From these observations, data was filtered according to three categories: (i) Highly abundant and consistent spots (detected in 6−8 groups); (ii), moderately abundant and variable (detected in 3−6 groups); and (iii), low abundance and most variable (detected in <3 groups). PDQuest, the software used in this analysis, is reported to have a reduced spot detection efficiency (70%) in regions of low signal-to-noise (i.e., low spot signal and high background noise),[19] resulting in increased detection of false positives and false negatives spots. This may in part explain the low level variation between TRAMs. Therefore, spots in group three (256 spots in total) were discarded from further analysis, as these were unlikely to be due to actual differences in TRAM protein content.

Characterizing the Protein Profiles of TRAM and Wash Medium. Considerable differences in the protein maps of TRAM and wash media made cross matching difficult (Figure 2). Typically, 62% of proteins detected in TRAM were also matched to wash media samples, suggesting protein elution occurred, but was variable and protein-specific. A recent report has suggested that many spots may in fact be the result of more than one protein comigrating, which in fact overlap.[20] Without further verification of matched proteins, one cannot therefore assume that matched spots between gels from different samples are actually derived from identical proteins. Realistically, matching such dissimilar samples cannot be performed confidently, and each gel must therefore be analyzed as a separate entity. For this reason, only representative gels were matched to assist in assessing the effect of handling on identified proteins.

Characterizing Proteins of TRAM. Spots resolved in TRAM (and in wash media to act as markers to cross gel matching) were selected for mass spectrometric identification. Peptides were subjected to MALDI-TOF−MS peptide mass fingerprint (PMF) analysis and/or ESI-Q-TOF−MS/MS (Tables 1 and 2, and Supporting Information Figures 1 and 2). Spots that could not be confidently matched, or identified using mass spectrometry techniques, were discarded from the analysis set. Approximately 20% of the proteins identified from TRAM 2-D gels exhibited charge heterogeneity (e.g., Spot 53). Such presence of different isoforms of the same protein, are most likely due to post-translational modifications (PTM), which are typically required to modify the biological activity of proteins.

Characterizing the Effect of Handling on Proteins of AM. Using Swiss-Prot, PUBMED and the Human Proteome Reference Database, identified proteins were classified according to sub-cellular compartmentalization and physiological function (Supporting Information Table 3). Also, proteins not previously identified in any mammalian AM using direct identification methods such as mass spectrometry are indicated. Thus, none of the proteins identified have been detected previously in mammalian AM by direct methods although some have been identified by indirect methods (antibody based). The proteins are categorized according to their predominant subcellular location and functions in current literature (Figure 3). Proteins detected in both TRAM and the wash media suggested that partial release of these proteins had occurred, which appeared to be on a protein specific basis (Table. 1, and Figure 3). These proteins were largely soluble cytoplasmic-related proteins (Figure 3, A, *CO*), which were also present in other insoluble forms, or were also compartmentalized, e.g., in mitochondria

Table 1. Proteins Affected by Handling; Detected in Both the TRAM and the Matched Wash Fraction

spot (additional)	protein name	acc. no.	mass spec method	M_r (kDa) observed/ theoretical	p*I* observed/ theoretical
1	Cofilin 1	P23528	MS/MS	16/18.5	7.8/8.2
2	Cyclophilin A	P62937	MS/MS	15/17.8	7.5/7.8
3	Hemoglobin alpha chain	P69905	MS/MS	15/15.1	8.1/8.3
5	Hemoglobin beta chain	P68871	MS/MS & PMF	15/16	7.1/7.2
7	Calpactin I[†]	P60903	MS/MS	12/11.1	7.2/7.3
8	Calgizzarin	P31949	MS/MS	11/11.7	6.4/6.5
9	Calcyclin	P06703	MS/MS	10/10.1	5.9/5.3
10	Calvasculin	P26447	MS/MS	11/11.8	5.9/5.8
11	Galectin I	P09382	MS/MS & PMF	13/14.6	5.7/5.3
12	Alpha Crystallin B chain	P02511	PMF	21/20.1	7/6.7
15	Phosphoglycerate mutase 1	P18669	PMF	28/28.7	6.8/6.7
16	Peroxiredoxin 6	P30041	PMF	26/25	6.2/6.0
17	Annexin A4	P09525	PMF	33/35.8	5.8/5.8
19	Mimecan [Precursor]	P20774	MS/MS & PMF	34/34	5.3/5.4
21	Thrombospondin 1	P07996	MS/MS & PMF	31/127.5	5.7/4.7
24 (20, 23)	Annexin II	P07355	MS/MS &PMF	36/38.5	7.3/7.6
25	Elongation Factor Tu	P49411	PMF	46/45	6.7/6.3
27 (26)	Alpha enolase	P06733	PMF	50/47	6.9/7.0
31	Septin 2	Q15019	PMF	45/41.5	6.3/6.2
32 (33)	HSRBC protein	Q969G5	PMF	41/27.6	5.8/59
36	Actin; Cytoplasmic Chain1	P60709	PMF	47/43	5.2/5.3
37	GRP58	P30101	PMF	58/54.2	5.8/5.6
41	4-PH alpha-1	P13674	PMF	62/59.1	5.9/5.7
43	Heat shock 70kDa protein 1	P08107	MS/MS & PMF	70/70.0	5.4/5.5
45	Protein disulfide-Isomerase	P07237	PMF	64/57	4.6/4.7
46	Vimentin	P08670	PMF	65/53.5	4.9/5.1
47	Keratin 24	Q9NXG7	PMF	59/55.6	4.9/4.9
48	Serum albumin precursor	P02768	PMF	70/66.4	5.9/5.7
49	Ezrin (villin 2)	P15311	PMF	77/69.2	6.3/5.9
55	Integrin alpha-6	P23229	MS/MS & PMF	105/101.7	4.3−5.6/5.5
56	Calreticulin precursor	P27797	MS/MS & PMF	49.4/67	4.3/4.3
57	Neutral alpha-glucosidase AB	Q14697	PMF	94/107	5.8/5.7
59 (14)	Triosephosphate isomerase 1	Q8WWD0	PMF	26/26.6	6.7/6.5
60	Glutathione S-transferase P	P09211	PMF	23.2/25	5.6/5.4
62	Thrombospondin-1 Precursor	P07996	PMF	31/127.5	5.3/4.7
63	Endoplasmin precursor	P14625	PMF	98/90.17	4.7/4.7
64	Macrophage capping protein	P40121	MS/MS & PMF	44/38.51	6.0/5.8
65 (22)	Annexin A1	P04083	PMF	38/38.5	6.4/6.6
66	Chain 2; Gelsolin	P06396	PMF	83/80.5	5.6/5.5
67	Chain 2; Gelsolin	P06396	PMF	83/80.5	5.7/5.5
69	Elongation Factor 2	P13639	PMF	93/95.2	6.9/6.4
70	Phosphoglycerate Kinase 1	P00558	PMF	43/44.4	8.2/8.3

[a] Calpactin I (spots 6 and 7) was represented by duplicate spots existing in more than one form. This resulted in one form of the protein being detected in both the wash media and TRAM, and one in the TRAM alone.

(*M*), endoplasmic reticulum (*ER*), or integral to membrane and "associated" with membrane structures (*MB*). The predominant function of these proteins serves to maintain, and modulate, the structure of the cell (*CS*), and maintain constitutive general cellular function and protein metabolism (Figure 3B). Proteins identified solely in TRAM (Table 2, and Figure 3, parts C and D) were primarily classified as cytoskeleton-related proteins (31%, Figure 3C), cell organelle (43%, Figure 3C), and extracellular related proteins (14%, Figure 3C). These were predominantly integral components of the cell structure (Figure 3D, *CS*) or functionality of the cell that were rendered insoluble during handling. These proteins were also identified as the most abundant and least variable spots, as defined above (Figure 1).

The elution of intracellular proteins was indicative of cell lysis. However, histology (Figure 4) and mass spectrometric identification of cell structural proteins solely in TRAM suggested that, although nonviable, the cells remained morphologically intact at a gross level and associated with the AM. This is further suggested by the identification of the epithelial hemidesmosomal protein integrin-α6 (Figure 2, and Table 1, spot 55) in TRAM.

Conventional protein mapping is typically undertaken on viable tissue or living cells. However, this work differs in that the biological tissue studied has been processed for use in an ectopic site as a nonviable construct/scaffold. Thus, any further consideration of the proteins present should be qualified accordingly. Although many intracellular proteins have been identified from nonliving epithelium, the subsequent focus of this research was to identify key proteins that can be implicated in the various putative clinical mechanisms of action of TRAM.

Identification of Potential Proteins of Interest in TRAM. Thrombospondin-1. The identification of thrombospondin-1 (TSP-1; Figure 2 Spots 21, and 62) in TRAM confirms TSP-1 expression in amnion cells.[21] TSP-1 participates in cell-to-cell and cell-to-matrix communication,[22] and has been implicated in the mediation of cellular adhesion, proliferation, differentiation, and migration, and also apoptosis.[23] More importantly, TSP-1 is reported to control a number of physiological processes such as wound repair, inflammatory response, and angiogenesis.[22,24]

Table 2. Proteins Unaffected by Handling; Identified in AM Alone

spot (additional)	protein name	acc. no.	mass spec method	M_r (kDa) observed/ theoretical	p*I* observed/ theoretical
6	Calpactin I [a]	P60903	MS/MS	12/11.0	7.4/7.3
13	Superoxide dismutase	P04179	PMF	21/22.2	7/6.7
18	60 kDa heat shock protein	P10809	PMF	64/57.9	5.2/5.2
28	Glutamate dehygrogenase 1	P00367	PMF	53/61	6.9/6.7
29	Ornithine aminotransferase, mitochondrial precursor	P04181	PMF	47/48	6.3/6.57
30	Keratin, type I cytokeratin 18	P05783	PMF	44/47.9	6.3/5.3
34	Keratin, type I cytoskeletal 19	P08727	MS/MS	45/44.1	4.9/5.1
35 (68)	Keratin, type II cytoskeletal 8	P05787	MS/MS	54/53.5	5.5/5.5
38	Keratin, type II cytoskeletal 6A	P02538	PMF	59/60	6.6/8.1
39	Keratin, type II cytoskeletal 6A	P02538	PMF	56/59.9	7.3/8.1
40	BIG-H3	Q15582	MS/MS & PMF	63/73.1	7.0/7.4
42	Keratin, type I cytoskeletal 17	Q04695	PMF	54/49	5.0/5.0
44	Heat shock 70kDa protein 9B	P38646	MS/MS & PMF	73/68.6	5.4/5.4
50	Lamin A/C	P02545	PMF	72−79/74.1	6.6−6.9/6.6
51	Citrate Hydrol-lyse	Q99798	PMF	79/82.4	7.0/6.9
52	pp-Ga1NAc-T5	Q7Z7M9	PMF	107/106.2	7.0−7.1/9.5
53	Collagen type VI α2(VI)	P12110	MS/MS & PMF	111/97.4	6.1−6.2/5.4
54	Collagen type VI α1(VI)	P12109	PMF	116/108.5	5.0/5.3
58	Flavin reductase	P30043	PMF	23/21.9	7.3/7.3

[a] Calpactin I (spots 6 and 7) was represented by duplicate spots existing in more than one form. This resulted in one form of the protein being detected in both the wash media and TRAM, and one in the TRAM alone.

Although mature TSP-1 monomers resolve around 127.5 kDa and p*I* 4.7, the spots identified as TSP-1 in TRAM consistently resolved at approximately 31 kDa, and p*I* 4.3 and 4.7. TSP-1 exists as a homo-trimer, with each monomer composed of several multifunctional domains, assigned separately to a specific physiological process.[22] To characterize the identified fragment, peptide masses and identified sequences were assigned to peptides from a theoretical tryptic digest, and sequence of mature TSP-1. The fragment mapped to the N-terminal heparin binding domain (HBD), amino acids 1−299, with a theoretical spot size and charge of 31.5kDa, p*I* 6.45 respectively (http://us.expasy.org/tools/peptide-mass.html), which corresponded to the observed position of the spots in TRAM. The spots were also detected in fresh AM (data not shown) and washes (Figure 5). Considering that TSP-1 is among the most abundant and consistent protein detected in TRAM, has been implicated as a major mediator in wound healing and angiogenesis, and the most abundant protein secreted by human cultured corneal epithelial cells (Manuscript in preparation), further investigation of this protein was considered appropriate.

To confirm the presence of TSP-1 and identify further fragments, Western blotting was carried out, detecting using a cocktail of antibodies for several domains of TSP-1. Immunodetection of TSP-1 stained a band corresponding to the identified fragment in all media and TRAM samples (except one, Figure 5, Lane 15), indicating its dual existence as a free solute and as an AM-associated form. The parent TSP-1 protein was also detected in most samples, which was also detected as both a free and AM-associated form (Figure 5). The absence of TSP-1 parent protein in the spongy layer supports TSP-1 being a component of the ECM milieu.[25] A 97-kDa band was detected in eluted fractions, but not fresh AM or TRAM, which corresponded to the size of the remaining TSP-1 fragment with the N-terminal fragment removed. This indicated that the N-terminal fragment detected by 2-DE is proteolytically cleaved from mature TSP-1, rather than synthesized as a truncated N-terminal fragment. The detection of additional bands of varying sizes, particularly in media and spongy layer samples, supports this and also suggests that TSP-1 is particularly susceptible to proteolysis. This may also explain why, occasionally, extensive protease degradation appeared to occur in some samples (Figure 5, AM1). Such bands were not detected in corresponding TRAM suggesting that most mature TSP-1 is ECM bound, which is then proteolytically digested to release soluble fragments of various sizes, leaving behind the ECM bound N-terminal fragment. These results indicated that limited proteolytic products are generated in vivo, prior to handling, and is a common event in normal AM, with proteolysis increasing during handling.[26]

Similar truncated N-terminal fragments of TSP-1 have been reported in vitro.[25,27−29] These are either products of alternative spliced mRNA transcripts from the TSP-1 gene, or protease digestion products.[28] However, our results support the latter, suggesting TSP-1 undergoes site specific and limited proteolysis.[25] More specifically, extracellular digestion with plasmin and thrombin generates similar fragments to the TSP-1 fragment observed in TRAM.[22] TSP-1 is also degraded through endocytosis, mediated by the N-terminal HBD and calreticulin.[22,30] Calreticulin was also identified in TRAM (Figure 2, and Table 1, Spot 56), and is reported to mediate the anti-adhesive activity of TSP-1.

TSP-1 fragments retain their respective domain functions, which may then elicit a fragment-dependent biological response. This suggests that the function of the TSP-1 and its fragments detected in TRAM may therefore be preserved. TSP-1 is a known inhibitor of angiogenesis.[31] In the eye, TSP-1 has been implicated in maintaining corneal avascularity[32] and angiogenic privilege.[33] TSP-1 has a dual angiogenic inhibitory function, either directly suppressing migration and inducing apoptosis of endothelial cells through TGF-β1 activation,[34,35] or by indirectly inhibiting the production of pro-angiogenic factors and blocking the access to co-receptors on the endothelial cell surface.[36] However, in ocular pathological conditions, such as trauma and inflammation, neovascularisation may occur. In addition, TSP-1 is also reported to be one of several factors involved in corneal wound healing and antiangiogenic activity of AM in ex vivo expansion of human limbo-corneal

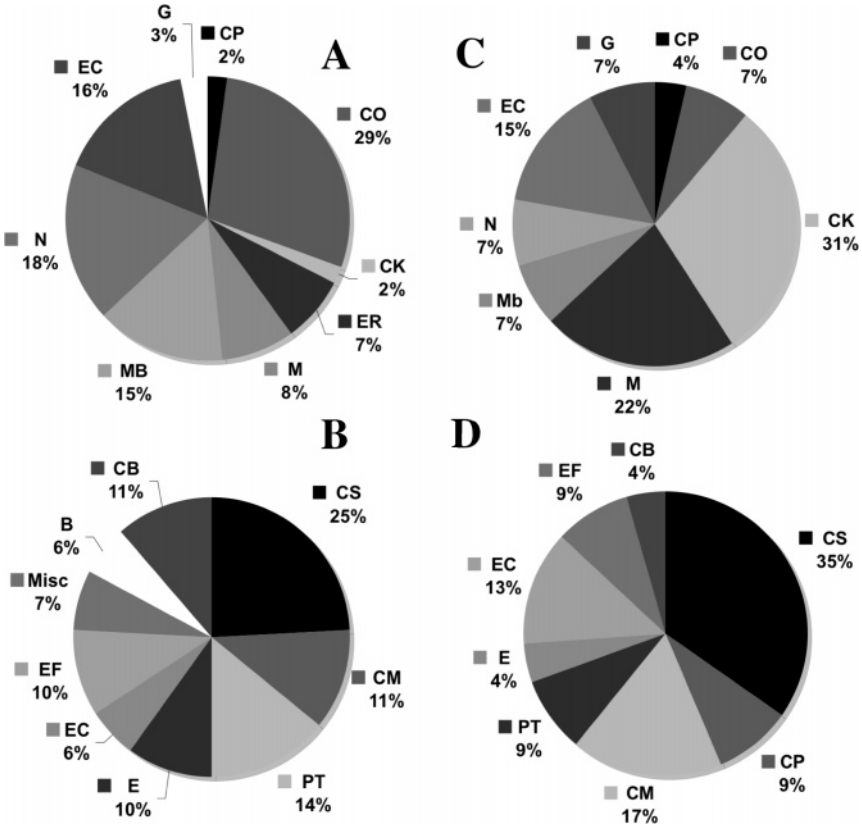

Figure 3. Distribution of proteins identified in the wash media (A & B), and TRAM only (C & D). Pie chart representing the distribution of all identified proteins in the proteome of both AM and wash media according to their sub-cellular location (A & C) and function (B & D). Assignments were made according to their predominant subcellular location and function as reported in the current literature and Swiss-Prot and Human Protein Reference (http://www.hprd.org/) databases. Subcellular location: (*CO*), Cytoplasm proteins with secondary subcellular locations; (*CP*), Cytoplasm only; (*CK*), Cytoplasmic cytoskeleton associated proteins; (*ER*), Endoplasmic reticulum; (*M*), Mitochondrion; (*MB*), Proteins integral to membrane and "associated" with membrane structure; (*N*), Nucleus, (*EC*), Protein found in the extracellular environment; (*G*), Golgi apparatus. Function: (*CS*), associated with maintaining and modulating cell structure; (*CP*), Functions associated with cell protection from free radicals and apoptosis; (*CM*), Functions associated with cellular metabolism; (*PT*), Protein folding/turnover; (*E*), Exocytosis; (*EC*), Functions associated with an extracellular processes; (*EF*), Intracellular protein with a secondary function when released extracellularly; (*CB*), Calcium ion binding protein; (*B*), classical blood/plasma proteins; (Misc), miscellaneous function including cell cycle, extracellular ligands and unknown.

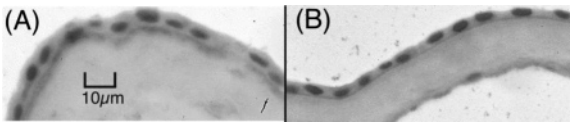

Figure 4. Effect of handling on AM structure and morphology. Segments of fresh (A) and corresponding AM preserved and prepared for transplantation (B), were sectioned and haematoxylin stained.

epithelial cells on AM.[37] TSP-1 may therefore play an important role in AM function, and further investigation of TSP-1 and the significance of proteolysis of TSP-1 are necessary.

Mimecan. Mimecan (Figure 2 and Table 1, Spot 19) is a small leucine-rich proteoglycan (SLRP), found in the ECM of connective tissue. Although previously unreported in AM, the detection of mimecan in TRAM supports the structural role in vivo, maintaining the tensile strength and hydrated nature of the tissue.[37,38] Mimecan is reported to be secreted and then proteolytically cleaved by a serine protease to form the 25-kDa ocular form.[39] Our results indicate that the larger form is present in TRAM, and is susceptible to proteolytic cleavage, which may explain the inter-membrane variation in spot intensity and abundance. Mimecan is one of the keratan sulfate-containing PGs reported to be involved in corneal architecture and transparency.[40,41] Corneal dystrophies and opaque corneal scars are associated with a lack of PGs, more specifically mimecan. Therefore, the presence of mimecan in AM may aid restoration of normal ocular function.

βIG-H3. βIG-H3 also known as TGFβI (TGF-β-induced gene-human, clone 3) or keratoepithelin[42] (Figure 2, spot 40), is an ECM adhesive molecule, constitutively expressed by many cell types.[40] It is among the most abundant and consistent proteins detected in AM, exhibiting extensive charge heterogeneity, suggesting the protein is post-translationally modified.[43] A recent report by Karring et al also demonstrated similar results in the cornea.[44] βIG-H3 acts as a membrane-associated growth factor during cell growth differentiation, and wound healing, particularly in the cornea.[45,46]

βIG-H3 is reported to covalently associate with collagen VI (an important ECM architectural protein) (Figure 2, spots 53 and 54), which mediates interactions with the cell surface via proteoglycan or integrins. This is particularly important in the cornea where collagen VI, βIG-H3, and proteoglycans have been immunolocalized with overlapping distributions.[40] The abnormal expression of βIG-H3 disrupts these normal interactions, and has been implicated in tissue pathology, more specifically

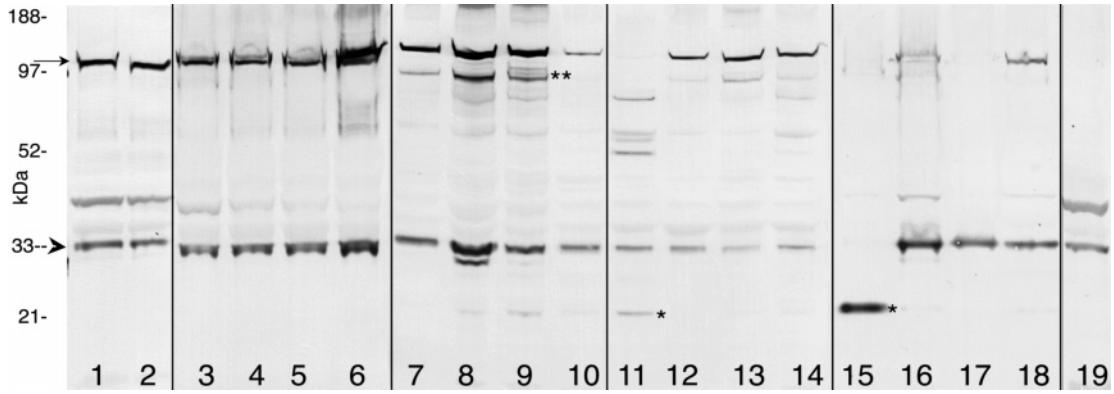

Figure 5. TSP-1 detection in AM. Total protein was assayed and 20 μg was loaded in each lane. Proteins were separated on denaturing PAGE mini-gels under reducing conditions, western blotted to PVDF and TSP-1 detected with anti-TSP antibody cocktail (AB-11, Neomarkers). Proteins were extracted from fresh AM (lanes 1,2), TRAM (lanes 3 to 6), storage medium (lanes 7 to 10), pooled wash media (lanes 11 to 14), spongy layer removed during processing (lanes 15 to 18), and chorion (lane 19). Samples shown correspond to four membranes; AM1 (lanes 1, 5, 9, 13, 17, and 18), AM2 (lanes 2, 6, 10, 14, and 19), AM3 (lanes 3, 7, 11, and 1) and AM4 (lanes 4, 8, 12, and 16). 127 kDa TSP-1 parent protein (Arrow), MS identified fragment (arrowhead), large fragment (**) and small fragment (*) are indicated. Size markers (Multimark, Invitrogen) are indicated. A representative experiment out of three performed is shown.

βIG-H3 related corneal dystrophies.[43,47] Therefore, βIG-H3 in TRAM may help to reinstate normal corneal function during wound repair.

Integrin α6. Integrin α6 (Figure 2, Spot 55) is a component of α6β4 integrin, predominantly expressed by a variety of epithelial cell types, and is the key hemidesmosomal protein involved in cell-to-matrix attachments. Although integrin α3β1 had been previously defined as the corneal epithelial receptor of βIG-H3, anti-α6 and anti-β4 integrin monoclonal antibodies block cell adhesions,[48] suggesting α6β4 integrin-βIG-H3 interaction is primarily responsible for cell attachment. Immunolocalization of integrin α6 in the corneal and amniotic BM supports this (data not shown). The integrin α6β4-βIG-H3 interaction plays an important role in mediating cell adhesion and wound repair signaling mechanisms;[48] therefore, AM may provide an ideal substrate for epithelial attachment and regrowth in the treatment of corneal epithelial dysfunction. This supports recent work reporting similarities in the architecture of AM and the ocular surface.[48]

Intracellular Proteins with an Extracellular Function. Intracellular proteins released from the cell following preservation are typically perceived as being of limited relevance to the clinical application of AM for wound repair. Nevertheless it is recognized that some of these proteins possess unintended functions in the extracellular environment. For example, heat shock proteins (HSPs) (Supplementary data, Table 3), released after cell death, or by secretion in response to stressful conditions have been reported to be pro-inflammatory.[49] HSP release might therefore be expected during AM handling and may have consequences related to AMT.

A number of properties have been attributed to extracellular annexins. Exogenous annexin A1 (Figure 2, spot 22) has been implicated as a mediator of the antiinflammatory response in several animal models reviewed by Gerke et al.,[50] and annexin A2 (Figure 2, spots 23 and 24) has been implicated in antithrombogenesis.[50] As annexins are among the most abundant proteins in TRAM, a biological effect seems likely, which may influence the functionality of AMT during wound healing, particularly in the eye.

Concluding Remarks

We have constructed a template reference map for proteins in TRAM. This will prove critical to the future understanding of the therapeutic mechanisms involved in AMT, especially in wound healing and regeneration. The identification of key proteins in TRAM such as active wound healing and anti-angiogenic mediators and those that mirror the architecture of the cornea goes some way to explaining its unique properties. Furthermore, the identification of AM components will assist in the efforts to generate bio-engineered and artificial AM constructs for surgical reconstruction. However, until such times, unless handling procedures are fully standardized, there will be variation in TRAM composition, which may ultimately compromise its therapeutic effect or lead to variability in clinical efficacy.

Acknowledgment. This work was supported by the Royal Blind Asylum and School/Scottish National Institution for the War Blinded, and Royal College of Surgeons Edinburgh, and in part by the Eye Research Institute Philadelphia, USA. Mass spectrometry was carried out by Matthew Carlile and Kevin Bailey, University of Nottingham Proteomics facility. Amniotic membranes were collected in collaboration with Professor D. K. James, Fetomaternal Medicine, University of Nottingham.

Supporting Information Available: (i) Data from spot analysis by PMF mass spectrometry and Mascot query; (ii) Data from peptide MS/MS sequencing and Mascot sequence query; and (iii) Details of proteins categorized according to function, location and previous identification in mammalian amniotic membrane. This material is available free of charge via the Internet at http://pubs.acs.org.

References

(1) Davis, J. W. Skin transplantation with a review of 550 cases at the Johns Hopkins Hospital. *Johns Hopkins Med. J.* **1910**, *15*, 307.
(2) Arnold, P. B.; Green, C. W.; Foresman, P. A.; Rodeheaver, G. T. Evaluation of resorbable barriers for preventing surgical adhesions. *Fertil. Steril.* **2000**, *73* (1), 157−161.

(3) Meek, M. F.; Coert, J. H.; Nicolai, J. P. Amnion tube for nerve regeneration. *Plast. Reconstr. Surg.* **2001**, *107* (2), 622−3.
(4) Goto, Y.; Noguchi, Y.; Nomura, A.; Sakamoto, T.; Ishii, Y.; Bitoh, S.; Picton, C.; Fujita, Y.; Watanabe, T.; Hasegawa, S.; Uchida, Y. In vitro reconstitution of the tracheal epithelium. *Am. J. Respir. Cell Mol. Biol.* **1999**, *20* (2), 312−318.
(5) Samandari, M. H.; Yaghmaei, M.; Ejlali, M.; Moshref, M.; Saffar, A. S. Use of amnion as a graft material in vestibuloplasty: a preliminary report. *Oral Surg. Oral Med. Oral Pathol. Oral Radiol. Endod.* **2004**, *97* (5), 574−578.
(6) Fishman, I. J.; Flores, F. N.; Scott, F. B.; Spjut, H. J.; Morrow, B. Use of fresh placental membranes for bladder reconstruction. *J. Urol.* **1987**, *138* (5), 1291−1294.
(7) Matthews, R. N. Human tissue response to amnion allograft. *Lancet* **1981**, *2* (8260−61), 1428.
(8) Hensle, T. W.; Seaman, E. K. Vaginal reconstruction in children and adults. *Technol. Urol.* **1995**, *1* (4), 174−180.
(9) Reim, M.; Redbrake, C.; Schrage, N. Chemical and thermal injuries of the eyes. Surgical and medical treatment based on clinical and pathophysiological findings. *Arch. Soc. Esp. Oftalmol.* **2001**, *76* (2), 103−124.
(10) Sheridan, R. L.; Moreno, C. Skin substitutes in burns. *Burns* **2001**, *27* (1), 92.
(11) Dua, H. S.; Gomes, J. A.; King, A. J.; Maharajan, V. S. The amniotic membrane in ophthalmology. *Surv. Ophthalmol.* **2004**, *49* (1), 51−77.
(12) Hopkinson, A.; McIntosh, R. S.; Tighe, P. J.; James, D. K.; Dua, H. S. Amniotic membrane for ocular surface reconstruction: Donor variations and handling affect membrane constituents. *IOVS* **2006**, In Press.
(13) Hopkinson, A.; McIntosh, R. S.; Layfield, R.; Keyte, J.; Dua, H. S.; Tighe, P. J. Optimised two-dimensional electrophoresis procedures for the protein characterisation of structural tissues. *Proteomics* **2005**, *5* (7), 1967−1979.
(14) Tsubota, K.; Shimazaki, J. Surgical treatment of children blinded by Stevens-Johnson syndrome. *Am. J. Ophthalmol.* **1999**, *128* (5), 573−581.
(15) Yan, J. X.; Wait, R.; Berkelman, T.; Harry, R. A.; Westbrook, J. A.; Wheeler, C. H.; Dunn, M. J. A modified silver staining protocol for visualization of proteins compatible with matrix-assisted laser desorption/ionization and electrospray ionization-mass spectrometry. *Electrophoresis* **2000**, *21* (17), 3666−3672.
(16) Rogers, M.; Graham, J.; Tonge, R. P. Statistical models of shape for the analysis of protein spots in two-dimensional electrophoresis gel images. *Proteomics* **2003**, *3* (6), 887−896.
(17) Shevchenko, A.; Wilm, M.; Vorm, O.; Mann, M., Mass spectrometric sequencing of proteins silver-stained polyacrylamide gels. *Anal. Chem.* **1996**, *68* (5), 850−858.
(18) Challapalli, K. K.; Zabel, C.; Schuchhardt, J.; Kaindl, A. M.; Klose, J.; Herzel, H. High reproducibility of large-gel two-dimensional electrophoresis. *Electrophoresis* **2004**, *25* (17), 3040−3047.
(19) Rogers, M.; Graham, J.; Tonge, R. P. Using statistical image models for objective evaluation of spot detection in two-dimensional gels. *Proteomics* **2003**, *3* (6), 879−886.
(20) Pietrogrande, M. C.; Marchetti, N.; Dondi, F.; Righetti, P. G. Spot overlapping in two-dimensional polyacrylamide gel electrophoresis maps: relevance to proteomics. *Electrophoresis* **2003**, *24* (1−2), 217−224.
(21) Hao, Y.; Ma, D. H.; Hwang, D. G.; Kim, W. S.; Zhang, F. Identification of antiangiogenic and antiinflammatory proteins in human amniotic membrane. *Cornea* **2000**, *19* (3), 348−352.
(22) Adams, J. C.; Lawler, J. The thrombospondins. *Int. J. Biochem. Cell Biol.* **2004**, *36* (6), 961−968.
(23) Clezardin, P.; Lawler, J.; Amiral, J.; Quentin, G.; Delmas, P., Identification of cell adhesive active sites in the N-terminal domain of thrombospondin-1. *Biochem. J.* **1997**, *321* (Pt 3), 819−827.
(24) Sid, B.; Sartelet, H.; Bellon, G.; El Btaouri, H.; Rath, G.; Delorme, N.; Haye, B.; Martiny, L. Thrombospondin 1: a multifunctional protein implicated in the regulation of tumor growth. *Crit. Rev. Oncol. Hematol.* **2004**, *49* (3), 245−258.
(25) Dixit, V. M.; Grant, G. A.; Santoro, S. A.; Frazier, W. A. Isolation and characterization of a heparin-binding domain from the amino terminus of platelet thrombospondin. *J. Biol. Chem.* **1984**, *259* (16), 10100−10105.
(26) Harder, A.; Wildgruber, R.; Nawrocki, A.; Fey, S. J.; Larsen, P. M.; Gorg, A., Comparison of yeast cell protein solubilization procedures for two-dimensional electrophoresis. *Electrophoresis* **1999**, *20* (4−5), 826−829.
(27) Sottile, J.; Selegue, J.; Mosher, D. F. Synthesis of truncated amino-terminal trimers of thrombospondin. *Biochemistry* **1991**, *30*, 0 (26), 6556−6562.
(28) Damas, C.; Vink, T.; Nieuwenhuis, H. K.; Sixma, J. J., The 33-kDa platelet alpha-granule membrane protein (GMP-33) is an N-terminal proteolytic fragment of thrombospondin. *Thromb. Haemost.* **2001**, *86* (3), 887−893.
(29) Yu, H.; Tyrrell, D.; Cashel, J.; Guo, N. H.; Vogel, T.; Sipes, J. M.; Lam, L.; Fillit, H. M.; Hartman, J.; Mendelovitz, S.; Panel, A.; Roberts, D. D., Specificities of heparin-binding sites from the amino-terminus and type 1 repeats of thrombospondin-1. *Arch. Biochem. Biophys.* **2000**, *374* (1), 13−23.
(30) Lawler, J. Thrombospondin-1 as an endogenous inhibitor of angiogenesis and tumor growth. *J. Cell Mol. Med.* **2002**, *6* (1), 1−12.
(31) Chen, H.; Herndon, M. E.; Lawler, J. The cell biology of thrombospondin-1. *Matrix. Biol.* **2000**, *19* (7), 597−614.
(32) Ma, D. H.; Yao, J. Y.; Yeh, L. K.; Liang, S. T.; See, L. C.; Chen, H. T.; Lin, K. Y.; Liang, C. C.; Lin, K. K.; Chen, J. K. In vitro antiangiogenic activity in ex vivo expanded human limbocorneal epithelial cells cultivated on human amniotic membrane. *Invest. Ophthalmol. Vis. Sci.* **2004**, *45* (8), 2586−2595.
(33) Uno, K.; Hayashi, H.; Kuroki, M.; Uchida, H.; Yamauchi, Y.; Oshima, K. Thrombospondin-1 accelerates wound healing of corneal epithelia. *Biochem. Biophys. Res. Commun.* **2004**, *315* (4), 928−934.
(34) Crawford, S. E.; Stellmach, V.; Murphy-Ullrich, J. E.; Ribeiro, S. M.; Lawler, J.; Hynes, R. O.; Boivin, G. P.; Bouck, N. Thrombospondin-1 is a major activator of TGF-beta1 in vivo. *Cell* **1998**, *93* (7), 1159−1170.
(35) Huang, Z.; Bao, S. D. Roles of main pro- and anti-angiogenic factors in tumor angiogenesis. *World J. Gastroenterol.* **2004**, *10* (4), 463−470.
(36) Funderburgh, J. L.; Funderburgh, M. L.; Mann, M. M.; Corpuz, L.; Roth, M. R. Proteoglycan expression during transforming growth factor beta -induced keratocyte-myofibroblast transdifferentiation. *J. Biol. Chem.* **2001**, *276* (47), 44173−44178.
(37) Funderburgh, J. L.; Corpuz, L. M.; Roth, M. R.; Funderburgh, M. L.; Tasheva, E. S.; Conrad, G. W. Mimecan, the 25-kDa corneal keratan sulfate proteoglycan, is a product of the gene producing osteoglycin. *J. Biol. Chem.* **1997**, *272* (44), 28089−28095.
(38) Tasheva, E. S.; Koester, A.; Paulsen, A. Q.; Garrett, A. S.; Boyle, D. L.; Davidson, H. J.; Song, M.; Fox, N.; Conrad, G. W. Mimecan/osteoglycin-deficient mice have collagen fibril abnormalities. *Mol. Vis.* **2002**, *8*, 407−415.
(39) Kocak-Altintas, A. G.; Kocak-Midillioglu, I.; Akarsu, A. N.; Duman, S. BIGH3 gene analysis in the differential diagnosis of corneal dystrophies. *Cornea* **2001**, *20* (1), 64−68.
(40) Kim, M. O.; Yun, S. J.; Kim, I. S.; Sohn, S.; Lee, E. H. Transforming growth factor-beta-inducible gene-h3 (beta(ig)-h3) promotes cell adhesion of human astrocytoma cells in vitro: implication of alpha6beta4 integrin. *Neurosci. Lett.* **2003**, *336* (2), 93−96.
(41) LeBaron, R. G.; Bezverkov, K. I.; Zimber, M. P.; Pavelec, R.; Skonier, J.; Purchio, A. F. Beta IG-H3, a novel secretory protein inducible by transforming growth factor-beta, is present in normal skin and promotes the adhesion and spreading of dermal fibroblasts in vitro. *J. Invest. Dermatol.* **1995**, *104* (5), 844−849.
(42) Escribano, J.; Hernando, N.; Ghosh, S.; Crabb, J.; Coca-Prados, M. cDNA from human ocular ciliary epithelium homologous to beta ig-h3 is preferentially expressed as an extracellular protein in the corneal epithelium. *J. Cell Physiol.* **1994**, *160* (3), 511−521.
(43) Munier, F. L.; Frueh, B. E.; Othenin-Girard, P.; Uffer, S.; Cousin, P.; Wang, M. X.; Heon, E.; Black, G. C.; Blasi, M. A.; Balestrazzi, E.; Lorenz, B.; Escoto, R.; Barraquer, R.; Hoeltzenbein, M.; Gloor, B.; Fossarello, M.; Singh, A. D.; Arsenijevic, Y.; Zografos, L.; Schorderet, D. F. BIGH3 mutation spectrum in corneal dystrophies. *Invest. Ophthalmol. Vis. Sci.* **2002**, *43* (4), 949−954.
(44) Karring, H.; Thogersen, I. B.; Klintworth, G. K.; Moller-Pedersen, T.; Enghild, J. J. A dataset of human cornea proteins identified by Peptide mass fingerprinting and tandem mass spectrometry. *Mol. Cell. Proteomics* **2005**, *4* (9), 1406−1408.

(45) Ha, S. W.; Bae, J. S.; Yeo, H. J.; Lee, S. H.; Choi, J. Y.; Sohn, Y. K.; Kim, J. G.; Kim, I. S.; Kim, B. W. TGF-beta-induced protein betaig-h3 is upregulated by high glucose in vascular smooth muscle cells. *J. Cell Biochem.* **2003**, *88* (4), 774−782.
(46) Hanssen, E.; Reinboth, B.; Gibson, M. A., Covalent and noncovalent interactions of {beta}ig-h3 with collagen VI.{beta}ig-h3 is covalently attached to the amino-terminal region of collagen VI in tissue microfibrils. *J. Biol. Chem.* **2003**.
(47) Klintworth, G. K.; Bao, W.; Afshari, N. A., Two mutations in the TGFBI (BIGH3) gene associated with lattice corneal dystrophy in an extensively studied family. *Invest. Ophthalmol. Vis. Sci.* **2004**, *45* (5), 1382−1388.
(48) Endo, K.; Nakamura, T.; Kawasaki, S.; Kinoshita, S. Human amniotic membrane, like corneal epithelial basement membrane, manifests the alpha5 chain of type IV collagen. *Invest. Ophthalmol. Vis. Sci.* **2004**, *45* (6), 1771−1774.
(49) Tsan, M. F.; Gao, B. Cytokine function of heat shock proteins. *Am. J. Physiol. Cell. Physiol.* **2004**, *286* (4), C739−744.
(50) Gerke, V.; Moss, S. E. Annexins: from structure to function. *Physiol. Rev.* **2002**, *82* (2), 331−371.

PR050425Q